

On the importance of neutral composition and temperature measurements in the 100-200 km altitude region

McArthur Jones Jr.^{1*}, John T. Emmert¹, Quan Gan², Jia Yue^{3, 4}

¹United States Naval Research Laboratory, United States, ²Laboratory for Atmospheric and Space Physics, University of Colorado Boulder, United States, ³Goddard Space Flight Center, National Aeronautics and Space Administration, United States, ⁴The Catholic University of America, United States

Submitted to Journal:
Frontiers in Astronomy and Space Sciences

Specialty Section:
Space Physics

Article type:
Brief Research Report Article

Manuscript ID:
1062967

Received on:
06 Oct 2022

Revised on:
26 Oct 2022

Journal website link:
www.frontiersin.org

Conflict of interest statement

The authors declare that the research was conducted in the absence of any commercial or financial relationships that could be construed as a potential conflict of interest

Author contribution statement

MJ and JTE equally contributed to this work, and share first authorship. All authors contributed to manuscript citations, revisions, reading, and approved the submitted version.

Keywords

thermosphere, Ionosphere, temperature, Mass density, composition, Space weather, Space climate

Abstract

Word count: 136

Currently, thermospheric species densities and temperatures between ~100-200 km are not known to the accuracy needed to fully characterize how the thermosphere transitions from a well-mixed atmosphere to a diffusively separated atmosphere with zero temperature gradient. This greatly inhibits scientific discovery attainable from either models or observations in this region, especially the understanding of mechanisms that drive thermosphere and ionospheric variability from space weather to climatological time scales. The purpose of this paper is to highlight the importance and critical need for new, global, height-resolved neutral composition (O, O₂, N₂) and temperature measurements in the new ignorosphere: the 100-200 km region of the thermosphere. We conclude with observation recommendations and requirements for new comprehensive composition and temperature measurements in the 100-200 km altitude region that would lead to significant advances in thermosphere-ionosphere science, space weather, and space climate.

Contribution to the field

The purpose of this brief research report is to highlight the importance and critical need for new, global, height-resolved neutral composition (O, O₂, N₂) and temperature measurements in the new ignorosphere: the 100-200 km region of the thermosphere. This article highlights the vertical extent and duration of past and current global thermospheric composition and temperature observations and provides a detailed scientific description on the urgent need for new global thermospheric observations in the all important 100-200 km region. This article closes by offering recommendations for addressing limitations in the "Ignorosphere" and "Thermospheric Gap" between 100-200 km.

Funding statement

MJ and JTE were supported by the Office of Naval Research. QG was supported by NASA grants 80NSSC20K0721 and 80GSFC18C006. JY was supported by NSF AGS-2140031, NASA, and the NASA AIM mission.

Ethics statements

Studies involving animal subjects

Generated Statement: No animal studies are presented in this manuscript.

Studies involving human subjects

Generated Statement: No human studies are presented in this manuscript.

Inclusion of identifiable human data

Generated Statement: No potentially identifiable human images or data is presented in this study.

Data availability statement

Generated Statement: Publicly available datasets were analyzed in this study. This data can be found here: NRLMSIS 2.0 Code and all data samples used in the ensemble fits and model validation are available at <https://map.nrl.navy.mil/map/pub/nrl/NRLMSIS/NRLMSIS2.0>. **Ground-based lidar and ISR data were obtained from <http://www.cedar.openmadrigal.org>** website. USU Lidar data are also available online (<https://doi.org/10.15142/T33H26>). MIPAS data used in this study are **available for registered users at <http://www.imk-asf.kit.edu/english/308.php> website. MIGHTI data used in this study** are available at available from the ICON website (<https://icon.ssl.berkeley.edu/Data>) and at the Space Physics Data Facility (<https://spdf.gsfc.nasa.gov/>)..

In review

On the importance of neutral composition and temperature measurements in the 100-200 km altitude region

1 **McArthur Jones Jr. ^{1,*}, John T. Emmert¹, Quan Gan², and Jia Yue^{3,4}**

2 ¹Space Science Division, U.S. Naval Research Laboratory, Washington, DC, USA.

3 ²Laboratory for Atmospheric and Space Physics, University of Colorado, Boulder, CO, USA.

4 ³Goddard Space Flight Center, NASA, Greenbelt, MD, USA.

5 ⁴Catholic University of America, Washington, DC, USA.

6 *** Correspondence:**

7 McArthur Jones Jr.

8 mcarthur.jones@nrl.navy.mil

9 **Keywords:** Thermosphere, Ionosphere, Temperature, Mass Density, Composition, Space
10 Weather, Space Climate

11 **Abstract**

12 Currently, thermospheric species densities and temperatures between ~100-200 km are not known to
13 the accuracy needed to fully characterize how the thermosphere transitions from a well-mixed
14 atmosphere to a diffusively separated atmosphere with zero temperature gradient. This greatly
15 inhibits scientific discovery attainable from either models or observations in this region, especially
16 the understanding of mechanisms that drive thermosphere and ionospheric variability from space
17 weather to climatological time scales. The purpose of this paper is to highlight the importance and
18 critical need for new, global, height-resolved neutral composition (O, O_2, N_2) and temperature
19 measurements in the new ignorosphere: the 100-200 km region of the thermosphere. We conclude
20 with observation recommendations and requirements for new comprehensive composition and
21 temperature measurements in the 100-200 km altitude region that would lead to significant advances
22 in thermosphere-ionosphere science, space weather, and space climate.

23 **1 Scientific Motivation and Challenges**

24 The thermosphere and ionosphere (T-I) system is forced from both above and below. From above,
25 external forcing includes (but is not limited to) extreme ultraviolet (EUV) and X-ray radiation as well
26 as energy and momentum input via coupling with the solar wind and magnetosphere. From below, a
27 wide-ranging spectrum of vertically propagating waves of lower atmospheric origin impart their
28 energy and momentum into the T-I system (Oberheide et al., 2015; Liu, 2016; Sassi et al., 2019).
29 Coupling between the plasma in the ionosphere and neutrals in thermosphere via ion drag, chemistry,
30 and Joule heating add even more complexity to T-I system. The primary neutral parameters that
31 define the thermospheric state are temperature, composition, mass density, and winds, which
32 experience variations over a wide range of spatiotemporal scales (e.g., Qian and Solomon, 2011;
33 Emmert et al., 2015) due to the energy and momentum inputs outlined above. Ultimately, neutral or
34 thermospheric variations, together with variations in the electrodynamic forcing, drive ionospheric
35 variations and produce the space weather of the T-I system (e.g., Rishbeth, 1998; Liu et al., 2021).

36 The thermosphere spans roughly 90-600 km altitude, consisting primarily of N₂, O₂, O, He, and H.
 37 The thermosphere transitions between ~100 and 120 km (e.g., Offermann et al., 2006) from a well-
 38 mixed fluid (dominated by eddy diffusion) to one dominated by molecular diffusion, whereby
 39 individual species are distributed by altitude according to their molecular masses. Above ~200 km,
 40 the thermosphere is in approximate diffusive equilibrium (Meier et al., 2001), transitioning from a
 41 molecular dominated atmosphere (N₂, O₂), to an atomic dominated regime, with O diffusing upward
 42 and becoming the major thermospheric species from ~200 to 600 km. Between ~250 and 750 km
 43 (depending on the solar cycle), O accounts for most of the thermospheric mass and therefore most of
 44 the atmospheric drag experienced by satellites and debris in low-Earth orbit. Critically, the O
 45 distribution in the mesosphere and lower thermosphere (MLT, ~50-120 km), which is controlled by
 46 the relative contributions of chemistry, diffusion, and dynamics (e.g., Yamazaki and Richmond,
 47 2013; Chang et al., 2014; Jones Jr., et al., 2014b; Gan et al., 2015), is directly connected to mass
 48 density distribution in the upper thermosphere via molecular diffusion (Picone et al., 2013, Jones Jr.
 49 et al., 2017; 2018; 2021).

50 Adding to the complexity of the 100-200 km region is that the thermospheric temperature profile
 51 increases steeply with altitude from ~250 K at 100 km to ~1000 K at 200 km (on average).
 52 Numerous competing heating and cooling processes govern the temperature of the thermosphere,
 53 including direct absorption of solar UV radiation, thermal interaction with the ionosphere,
 54 exothermic chemical reactions, infrared radiation by several species (including CO₂ and NO), and
 55 adiabatic heating and cooling due to dynamic motions. The connection between temperature and
 56 mass density (and therefore composition) is via hydrostatic balance and the ideal gas law. Variations
 57 in mass density are highly sensitive to variations in underlying temperature because increased
 58 temperature acts to expand a hydrostatic column, leading to increases in the density scale height and
 59 increased mass density at a fixed altitude. For example, a 20 K overestimate of temperature over a 10
 60 km altitude band near 100 km will produce a ~20% overestimate of atmospheric density at higher
 61 altitudes, because the erroneously high temperature produces a more expanded air column via
 62 hydrostatic adjustment. Thus, in order to properly interpret mass and plasma density changes
 63 measured in the upper thermosphere from previous (e.g., Challenging Minisatellite Payload
 64 (CHAMP)) and future (e.g., Global Dynamics Constellation (GDC)) satellite missions, one must
 65 understand the temperature and composition of the 100-200 km region.

66 Further complicating the understanding of upper T-I variations connected with variations in the 100-
 67 200 km altitude regime is that most vertically-propagating waves (solar and lunar tides, planetary
 68 waves, Kelvin waves, gravity waves) break, dissipate, and generate secondary or higher order waves
 69 at this altitude, bringing momentum and energy from the lower atmosphere into the thermosphere. As
 70 a result, accurate modeling of neutral thermospheric composition, temperature, and ionospheric
 71 plasma density are important for satellite operations and requires a deft understanding of atmospheric
 72 waves, dynamics, and thermodynamics that modulate the neutral and plasma densities at time scales
 73 from days, months, years, to decades (e.g., Leonard et al., 2012; Qian et al., 2009, 2013; Vadas et al.,
 74 2014; Emmert, 2015; Pedatella et al., 2016; Thayer et al., 2021). Further, wave propagation and
 75 dissipation prior to geomagnetic storms can serve to precondition thermospheric composition,
 76 dynamics, and temperature, which if unaccounted for can lead to large uncertainties in modeled
 77 plasma density calculations (e.g., Pedatella et al. 2018).

78 All the above is well supported by a rich body of scientific literature and provided strong motivation
 79 for the GDC and Dynamical Neutral Atmosphere (DYNAMIC) science missions that were among
 80 the highest priority recommendations in the 2013 Decadal Survey (NRC, 2013). Further, both GDC
 81 and DYNAMIC were strongly advocated for in the Decadal Survey Midterm Assessment (NASEM,

82 2020), with the latter receiving strong community support from the 2022 CEDAR community
 83 statements on DYNAMIC (CEDAR, 2022).

84 **2 Current State of Temperature and Composition Measurements in the 100-200 km**

85 Sophisticated whole atmosphere and/or middle and upper atmospheric models constrained with
 86 realistic lower atmosphere forcing from atmospheric prediction systems or reanalyses can reproduce
 87 some of the nuances of T-I composition and temperature in the T-I system. Since the 2013 Decadal
 88 Survey, a number of advances in understanding the composition and temperature variations in the
 89 100-200 km region have been accomplished via combined data-modeling efforts.

90 However, temperature and composition measurements in the 100–200 km region are still very sparse,
 91 which is an obstacle to the validation and interpretation of the modeling results. Figure 1 illustrates
 92 the historical and current record of major data sets as a function of altitude and year. The only current
 93 and ongoing research measurements of major thermospheric chemical constituents and/or
 94 temperature above 105 km are from the NASA Ionospheric Connection Explore (ICON) mission
 95 (Immel et al., 2018; neutral temperature measurements only, max altitude 127 km daytime, 108 km
 96 nighttime), the NASA Global-scale Observations of the Limb and Disk (GOLD) mission (Eastes et
 97 al., 2017; temperature, a vertically integrated measurement that is of limited utility; column O/N₂ and
 98 O₂ vertical profiles, but in geostationary orbit, with limited longitudinal coverage), ground-based
 99 incoherent scatter radar (campaign-based operation, only ~3 sites, daytime only, requires special
 100 processing), ground-based airglow measurements (only at ~250 km altitude, nighttime, limited
 101 geographic coverage, sporadic temporal coverage), and ground-based resonance fluorescence lidars
 102 routinely measure temperature from ~ 80 km up to ~115 km at nighttime (Yuan et al., 2021), with
 103 occasional temperature observations reaching ~ 140 km and above (Liu et al., 2016 and Chu et al.,
 104 2011). Further, important for improving the Mass Spectrometer Incoherent Scatter radar or MSIS
 105 series of empirical models with current and future thermospheric composition and temperature
 106 measurements, is the complicating factor that measurement techniques often use MSIS itself as an
 107 initial guess or for ancillary parameters needed in the retrieval (e.g., Michelson Interferometer for
 108 Passive Atmospheric Sounding (MIPAS), Bermejo-Pantaleón et al., 2011; Global Ultraviolet Imager
 109 (GUVI), Meier et al., 2015). Thus, there is a need to expand existing and develop new techniques for
 110 measuring and retrieving thermospheric temperature and composition, especially between the 100 km
 111 and 200 km altitude region, which has strong vertical gradients and a strong influence on higher
 112 altitudes in the T-I.

113 In the absence of well-resolved global temperature and composition measurements the community
 114 has often turned to the empirical Mass Spectrometer Incoherent Scatter Radar (MSIS[®]) class of
 115 models (Hedin et al., 1977a;1997b; Hedin, 1987;1991; Picone et al., 2002) to understand and validate
 116 thermospheric composition and temperature phenomena in the 100-200 km region. MSIS recently
 117 went through a major reformulation and upgrade from NRLMSISE-00 to NRLMSIS version 2.0 by
 118 Emmert et al. (2020), using extensive new datasets from the ground to ~100 km altitude (green box
 119 labeled “Various Remote Sensing Observations”, post-2000 in Figure 1). Further, above ~250 km
 120 new satellite drag-derived mass densities were used to tune and recalibrate thermospheric atomic
 121 oxygen. Otherwise, the neutral parameters provided by the NRLMSISE-00 model in the
 122 thermosphere was largely retained. Emmert et al. (2020) specifically highlighted the scarcity of
 123 thermospheric composition and temperature measurements between 100-200 km, making the
 124 following statements, “*We also note that species densities in the middle thermosphere are not known*
 125 *to the accuracy needed to fully understand the critical transition from a fully mixed atmosphere to a*
 126 *diffusively separated one. Observations needed to constrain lower and middle thermospheric physics*

127 are scarce, and the 100–200 km region can perhaps be termed the new “ignorosphere,” an epithet
 128 previously applied to the mesosphere, which by comparison is now well measured and understood.”

129 Not only are thermospheric composition and temperature measurements sparse in the 100–200 km
 130 altitude region, but also existing temperature datasets exhibit large mutual biases of up to 80 K or
 131 more. For example, Figure 2 illustrates the mutual biases of selected thermospheric temperature data
 132 sets using NRLMSIS 2.0 as a benchmark, during the daytime and at mid-latitudes. Compounding the
 133 challenge of understanding the thermospheric state between 100–200 km and its impact on the
 134 overlying T-I system is that new “ignorosphere” overlaps the same altitude regime of the so-called
 135 “thermospheric gap”, a term coined by Oberheide et al. (2011). The “thermospheric gap” refers to
 136 110–200 km region of the thermosphere, where we know very little about the dynamics of this region
 137 due to a lack of vector wind measurements.

138 This lack of wind measurements coupled with the sparsity of composition and temperature
 139 measurements in the new ignorosphere has significantly hindered scientific progress on a number of
 140 T-I phenomena in which composition and temperature variations, and dynamical-control thereof, are
 141 known to play an important role. Just a few phenomena that cover both local and global spatial
 142 scales, as well as span time scales from days to beyond a solar cycle are listed below:

- 143 • Long-term trends in composition, mass density, and temperature in the thermosphere
 144 (Emmert, 2015; Solomon et al., 2019)
- 145 • The residual interhemispheric lower thermospheric residual circulation and its effect on O
 146 and temperature (Qian and Yue, 2017).
- 147 • Characterizing the prominent drivers (especially those associated with gravity waves and
 148 tides) of the global annual and semiannual oscillations in the upper T-I, and their solar cycle
 149 variability (Jones Jr. et al., 2021)
- 150 • The equinox transition of composition and temperature in the thermosphere (Qian et al.,
 151 2022).
- 152 • What actually causes changes in $\Sigma O/N_2$ in existing FUV measurements, be it O, N₂, or
 153 temperature and what is the contribution of each?
- 154 • Impacts of short-term (<5 days) variability of neutral constituents and temperature (e.g., Yue
 155 et al., 2016; Gan et al., 2017) between 100–200 km on the space weather of the upper T-I
 156 system.

157 3 Recommendations for Addressing Limitations in the “Ignorosphere” and 158 “Thermospheric Gap”

159 In the next decade, it is imperative that new and more extensive composition and temperature
 160 observations coupled with neutral wind measurements in the ignorosphere and thermospheric gap
 161 become available. Considering the scientific challenges listed above (and a number of others),
 162 Emmert et al. (2020) provided some recommendation on how to address such challenges including:

- 163 • New in situ mass spectrometers measurements of species densities in the thermosphere.
- 164 • New remote sensing (and potentially in situ) techniques for, and extensive new
 165 measurements, of height-resolved temperature and composition in the 100–200 km (and even
 166 slightly above) region.
- 167 • Dedicated research effort into identifying, characterizing, and reconciling systemic biases
 168 among existing and future composition and temperature observations.

169 Given these previous recommendations by Emmert et al. (2020) and others, we highly recommend
 170 flying a satellite constellation of at least 2 satellites, but ideally 3, with the necessary instruments that

would provide unprecedented longitude, local time, and height-resolved temperature and composition observations of the 100-200 km region. Table 1 provides a synopsis of the new thermospheric composition and temperature observations that would facilitate new scientific discoveries in the 100-200 km region of the thermosphere. Note that these composition and temperature measurements are not much different to what was advocated for in the 2013 Decadal Survey (NRC, 2013) when the DYNAMIC mission was originally proposed.

Additionally, the measurements in Table 1 coupled with coincident vector wind measurements at 4 local solar times per day (2 satellites separated apart by 6 hours) at the same resolution would allow one to resolve the large-scale gravity wave spectrum, daily diurnal tidal spectrum, and zonal mean wind daily. These waves are known to have profound effects on the thermospheric composition and temperature between 100-200 km and above (e.g., Yamazaki and Richmond, 2013; Jones Jr. et al., 2014a; Vadas et al., 2014). Ideally, the composition and temperatures measurements in Table 1 coupled with coincident vector wind measurements would be measured at 6 local solar times per day (3 satellites separated apart by 4 hours) at the same resolution, allowing one to resolve the daily semidiurnal tidal spectrum as well, in the altitude regime where many of these tides reach their maximum amplitude (e.g., Forbes et al., 2022). Observing the semidiurnal part of the tidal spectrum would add significant benefit as it is well-known to be important in coupling lower atmospheric variability to T-I variability in composition and temperature during sudden variability in composition and temperature during sudden stratospheric warmings (e.g., Jones Jr. et al. 2020; Oberheide et al., 2020; and many others before and after these).

In closing, the lack of global, day and night, height-resolved thermospheric composition and temperature (and wind) observations between 100 and 200 km has not been sufficiently addressed since the last Decadal Survey, and continues to be an important priority for the Heliophysics community. New, comprehensive, thermospheric composition and temperature (and wind) measurements in this altitude region, would significantly advance T-I system science, space weather modeling and prediction, and provide a means for more collaboration between the ground and space-based observation communities of the 100-200 km region. A table of other Heliophysics professionals that support our position on the future of thermospheric measurements in the 100-200 km region is included as supplementary material.

CONFLICT OF INTEREST

The authors declare that the research was conducted in the absence of any commercial or financial relationships that could be construed as a potential conflict of interest.

AUTHOR CONTRIBUTIONS

MJ and JTE equally contributed to this work, and share first authorship. All authors contributed to manuscript citations, revisions, reading, and approved the submitted version.

FUNDING

MJ and JTE were supported by the Office of Naval Research. QG was supported by NASA grants 80NSSC20K0721 and 80GSFC18C006. JY was supported by NSF AGS-2140031, NASA, and the NASA AIM mission.

ACKNOWLEDGMENTS

211 A similar version of this paper was submitted as a position paper to the Decadal Survey for Solar and
 212 Space Physics (Heliophysics) 2024-2033. The positions, experiences, and viewpoints expressed in
 213 this work are those of the authors as scientists in the space research community, and are not the
 214 official positions of their employing institutions. The authors would also like to thank Michael
 215 Stevens, Kenneth Dymond, and Andrew Stephan of NRL for their inputs on an initial version of this
 216 manuscript.

217 **DATA AVAILABILITY STATEMENT**

218 NRLMSIS 2.0 Code and all data samples used in the ensemble fits and model validation are available
 219 at <https://map.nrl.navy.mil/map/pub/nrl/NRLMSIS/NRLMSIS2.0>. Ground-based lidar and ISR data
 220 were obtained from <http://www.cedar.openmadrigal.org> website. USU Lidar data are also available
 221 online (<https://doi.org/10.15142/T33H26>). MIPAS data used in this study are available for registered
 222 users at <http://www.imk-asf.kit.edu/english/308.php> website. MIGHTI data used in this study are
 223 available at available from the ICON website (<https://icon.ssl.berkeley.edu/Data>) and at the Space
 224 Physics Data Facility (<https://spdf.gsfc.nasa.gov/>).

225 **REFERENCES**

226 Bermejo-Pantaleón, D., Funke, B., López-Puertas, M., García-Comas, M., Stiller, G., Clarmann, T.,
 227 Linden, A., Grabowski, U., Höpfner, M., Kiefer, M., Glatthor, N., Kellmann, S., and Lu, G. 2011.
 228 Global observations of thermospheric temperature and nitric oxide from MIPAS spectra at
 229 $5.3\mu\text{m}$. *Journal of Geophysical Research: Space Physics*, 116(A10). doi:
 230 <https://doi.org/10.1029/2011JA016752>.

231 (CEDAR) CEDAR Science Steering Committee. (2022). Cedar CSSC Community statement on
 232 DYNAMIC. Available at
 233 <https://docs.google.com/document/d/1J4zc0c4u0PCNJxPv1GFRKrgqDJN6mIQx/edit>.

234 Chang, L., Yue, J., Wang, W., Wu, Q., and Meier, R. 2014. Quasi two day wave-related variability in
 235 the background dynamics and composition of the mesosphere/thermosphere and the
 236 ionosphere. *Journal of Geophysical Research: Space Physics*, 119(6), p.4786-4804. doi:
 237 [10.1002/2014ja019936](https://doi.org/10.1002/2014ja019936).

238 Chu, X., Yu, Z., Gardner, C., Chen, C., and Fong, W. 2011. Lidar observations of neutral Fe layers
 239 and fast gravity waves in the thermosphere (110-155 km) at McMurdo (77.8°S, 166.7°E),
 240 Antarctica. *Geophysical Research Letters*, 38(23). doi:[10.1029/2011GL050016](https://doi.org/10.1029/2011GL050016).

241 Eastes, R., McClintonck, W., Burns, A., Anderson, D., Andersson, L., Codrescu, M., Correira, J.,
 242 Daniell, R., England, S., Evans, J., Harvey, J., Krywonos, A., Lumpe, J., Richmond, A., Rusch,
 243 D., Siegmund, O., Solomon, S., Strickland, D., Woods, T., Aksnes, A., Budzien, S., Dymond, K.,
 244 Eparvier, F., Martinis, C., and Oberheide, J. 2017. The Global-Scale Observations of the Limb
 245 and Disk (GOLD) Mission. *Space Science Reviews*, 212(1), p.383–408. doi:[10.1007/s11214-017-0392-2](https://doi.org/10.1007/s11214-017-0392-2).

247 Emmert, J. T. 2015. Altitude and solar activity dependence of 1967-2005 thermospheric density
 248 trends derived from orbital drag. *Journal of Geophysical Research: Space Physics*, 120(4),
 249 p.2940-2950. doi: [10.1002/2015JA021047](https://doi.org/10.1002/2015JA021047).

250 Emmert, J. T. 2015. Thermospheric mass density: A review. *Advances in Space Research*, 56(5),
 251 p.773-824. doi: <https://doi.org/10.1016/j.asr.2015.05.038>.

252 Emmert, J., Drob, D., Picone, J., Siskind, D., Jones Jr., M., Mlynczak, M., and et al. 2021. NRLMSIS
 253 2.0: A whole-atmosphere empirical model of temperature and neutral species densities. *Earth and
 254 Space Science*, 8(3), p.e2020EA001321. doi: <https://doi.org/10.1029/2020EA001321>.

255 Forbes, J., Oberheide, J., Zhang, X., Cullens, C., Englert, C., Harding, B., Harlander, J., Marr, K.,
 256 Makela, J., and Immel, T. 2022. Vertical Coupling by Solar Semidiurnal Tides in the
 257 Thermosphere From ICON/MIGHTI Measurements. *Journal of Geophysical Research: Space*
 258 *Physics*, 127(5), p.e2022JA030288. doi:10.1029/2022JA030288.

259 Gan, Q., Oberheide, J., Yue, J., and Wang, W. 2017. Short-term variability in the ionosphere due to
 260 the nonlinear interaction between the 6 day wave and migrating tides. *Journal of Geophysical*
 261 *Research: Space Physics*, 122(8), p.8831-8846. doi:10.1002/2017JA023947.

262 Gan, Q., Yue, J., Chang, L., Wang, W., Zhang, S., and Du, J. 2015. Observations of thermosphere
 263 and ionosphere changes due to the dissipative 6.5-day wave in the lower thermosphere. *Annales*
 264 *Geophysicae*, 33(7), p.913–922. doi:10.5194/angeo-33-913-2015

265 Hedin, A. 1987. MSIS-86 Thermospheric Model. *J. Geophys. Res. Space Physics*, 92(A5), p.4649-
 266 4662. doi:10.1029/JA092iA05p04649.

267 Hedin, A. 1991. Extension of the MSIS Thermosphere Model into the middle and lower
 268 atmosphere. *J. Geophys. Res. Space Physics*, 96(A2), p.1159-1172. doi:10.1029/90JA02125.

269 Hedin, A., Reber, C., Newton, G., Spencer, N., Brinton, H., Mayr, H., and Potter, W. 1977b. A global
 270 thermospheric model based on mass spectrometer and incoherent scatter data MSIS, 2.
 271 Composition. *J. Geophys. Res.*, 82(16), p.2148-2156. doi:10.1029/JA082i016p02148.

272 Hedin, A., Salah, J., Evans, J., Reber, C., Newton, G., Spencer, N., Kayser, D., Alcayd, D., Bauer,
 273 L., and McClure, J. 1977a. A global thermospheric model based on mass spectrometer and
 274 incoherent scatter data MSIS, 1. N₂ density and temperature. *J. Geophys. Res.*, 82(16), p.2139-
 275 2147. doi:10.1029/JA082i016p02139.

276 Immel, T., England, S., Mende, S., Heelis, R., Englert, C., Edelstein, J., Frey, H., Korpela, E., Taylor,
 277 E., Craig, W., Harris, S., Bester, M., Bust, G., Crowley, G., Forbes, J., Gerard, J.C., Harlander, J.,
 278 Huba, J., Hubert, B., Kamalabadi, F., Makela, J., Maute, A., Meier, R., Raftery, C., Rochus, P.,
 279 Siegmund, O., Stephan, A., Swenson, G., Frey, S., Hysell, D., Saito, A., Rider, K., and Sirk, M.
 280 2017. The Ionospheric Connection Explorer Mission: Mission Goals and Design. *Space Science*
 281 *Reviews*, 214(1), p.13. doi:10.1007/s11214-017-0449-2.

282 Jones Jr., M., Emmert, J., Drob, D., and Siskind, D. 2017. Middle atmosphere dynamical sources of
 283 the semiannual oscillation in the thermosphere and ionosphere. *Geophysical Research Letters*,
 284 44(1), p.12-21. doi: <https://doi.org/10.1002/2016GL071741>.

285 Jones Jr., M., Emmert, J., Drob, D., Picone, J., and Meier, R. 2018. Origins of the Thermosphere-
 286 Ionosphere Semiannual Oscillation: Reformulating the "Thermospheric Spoon"
 287 Mechanism. *Journal of Geophysical Research: Space Physics*, 123(1), p.931-954. doi:
 288 <https://doi.org/10.1002/2017JA024861>.

289 Jones Jr., M., Siskind, D., Drob, D., McCormack, J., Emmert, J., Dhadly, M., Attard, H., Mlynczak,
 290 M., Brown, P., Stober, G., Kozlovsky, A., Lester, M., and Jacobi, C. 2020. Coupling From the
 291 Middle Atmosphere to the Exobase: Dynamical Disturbance Effects on Light Chemical
 292 Species. *Journal of Geophysical Research: Space Physics*, 125(10). Doi:
 293 <https://doi.org/10.1029/2020JA028331>.

294 Jones Jr., M., Sutton, E., Emmert, J., Siskind, D., and Drob, D. 2021. On the Effects of Mesospheric
 295 and Lower Thermospheric Oxygen Chemistry on the Thermosphere and Ionosphere Semiannual
 296 Oscillation. *Journal of Geophysical Research: Space Physics*, 126(3). doi:
 297 <https://doi.org/10.1029/2020JA028647>.

298 Jones, M., Forbes, J., and Hagan, M. 2014b. Tidal-induced net transport effects on the oxygen
 299 distribution in the thermosphere. *Geophysical Research Letters*, 41(14), p.5272–5279.
 300 doi:10.1002/2014GL060698.

301 Jones, M., Forbes, J., Hagan, M., and Maute, A. 2014a. Impacts of vertically propagating tides on the
 302 mean state of the ionosphere-thermosphere system. *Journal of Geophysical Research: Space*
 303 *Physics*, 119(3), p.2197-2213. doi:10.1002/2013JA019744.

304 Leonard, J., Forbes, J., and Born, G. 2012. Impact of tidal density variability on orbital and reentry
 305 predictions. *Space Weather*, 10(12). doi:10.1029/2012SW000842.

306 Liu, A., Guo, Y., Vargas, F., and Swenson, G. 2016. First measurement of horizontal wind and
 307 temperature in the lower thermosphere (105-140 km) with a Na Lidar at Andes Lidar
 308 Observatory. *Geophysical Research Letters*, 43(6), p.2374-2380. doi:10.1002/2016GL068461.

309 Liu, H. -L. 2016. Variability and predictability of the space environment as related to lower
 310 atmosphere forcing. *Space Weather*, 14(9), p.634-658. doi:
 311 <https://doi.org/10.1002/2016SW001450>.

312 Liu, H., Yamazaki, Y., and Lei, J. (2021) 'Day-to-Day Variability of the Thermosphere and
 313 Ionosphere', *Upper Atmosphere Dynamics and Energetics*. American Geophysical Union (AGU),
 314 σσ. 275–300. doi: 10.1002/9781119815631.ch15. doi:
 315 <https://doi.org/10.1002/9781119815631.ch15>.

316 Meier, R., Picone, J., Drob, D., and Roble, R. 2001. Similarity transformation-based analysis of
 317 atmospheric models, data, and inverse remote sensing algorithms. *Journal of Geophysical
 318 Research: Space Physics*, 106(A8), p.15519-15532. doi:10.1029/2001JA000062.

319 Meier, R., Picone, J., Drob, D., Bishop, J., Emmert, J., Lean, J., Stephan, A., Strickland, D.,
 320 Christensen, A., Paxton, L., Morrison, D., Kil, H., Wolven, B., Woods, T., Crowley, G., and
 321 Gibson, S. 2015. Remote Sensing of Earth's Limb by TIMED/GUVI: Retrieval of thermospheric
 322 composition and temperature. *Earth and Space Science*, 2(1), p.1-37. doi:
 323 <https://doi.org/10.1002/2014EA000035>.

324 (NASEM) National Academies of Sciences, Engineering, and Medicine. 2020. *Progress Toward
 325 Implementation of the 2013 Decadal Survey for Solar and Space Physics: A Midterm Assessment*.
 326 The National Academies Press. doi:10.17226/25668

327 (NRC) National Research Council. 2013. *Solar and Space Physics: A Science for a Technological
 328 Society*. The National Academies Press. doi: 10.17226/13060

329 Oberheide, J., Forbes, J. M., Zhang, X., and Bruinsma, S. L. 2011. Climatology of upward
 330 propagating diurnal and semidiurnal tides in the thermosphere. *J. Geophys. Res. Space Physics*,
 331 116(A11). doi:10.1029/2011JA016784

332 Oberheide, J., Pedatella, N., Gan, Q., Kumari, K., Burns, A., and Eastes, R. 2020. Thermospheric
 333 Composition O/N₂ Response to an Altered Meridional Mean Circulation During Sudden
 334 Stratospheric Warmings Observed by GOLD. *Geophysical Research Letters*, 47(1). doi:
 335 <https://doi.org/10.1029/2019GL086313>.

336 Oberheide, J., Shiokawa, K., Gurubaran, S., Ward, W., Fujiwara, H., Kosch, M., Makela, J., and
 337 Takahashi, H. 2015. The geospace response to variable inputs from the lower atmosphere: a
 338 review of the progress made by Task Group 4 of CAWSES-II. *Progress in Earth and Planetary
 339 Science*, 2(1), p.2. doi:10.1186/s40645-014-0031-4.

340 Offermann, D., Jarisch, J., Schmidt, H., Oberheide, J., Grossmann, K. U., Gusev, O., Russell, J. M.
 341 III, and Mlynczak, M. G. 2007. The "wave turbopause". *Journal of Atmospheric and Solar-
 342 Terrestrial Physics*, 69(17), p.2139-2158.

343 Pedatella, N., and Liu, H.L. 2018. The Influence of Internal Atmospheric Variability on the
 344 Ionosphere Response to a Geomagnetic Storm. *Geophysical Research Letters*, 45(10), p.4578-
 345 4585. doi: <https://doi.org/10.1029/2018GL077867>.

346 Pedatella, N., Oberheide, J., Sutton, E., Liu, H.L., Anderson, J., and Raeder, K. 2016. Short-term
 347 nonmigrating tide variability in the mesosphere, thermosphere, and ionosphere. *Journal of
 348 Geophysical Research: Space Physics*, 121(4), p.3621-3633. doi:10.1002/2016JA022528.

349 Picone, J. M., Hedin, A. E., Drob, D. P., and Aikin, A. C. 2002. NRLMSISE-00 empirical model of
 350 the atmosphere: Statistical comparisons and scientific issues. *J. Geophys. Res. Space Physics*,
 351 107(A12), p.SIA 15-1–SIA 15-16. doi:10.1029/2002JA009430

352 Picone, J. M., Meier, R. R., and Emmert, J. T. 2013. Theoretical tools for studies of low-frequency
 353 thermospheric variability. *J. Geophys. Res. Space Physics*, 118(9), p.5853-5873. doi:
 354 <https://doi.org/10.1002/jgra.50472>.

355 Qian, L., and Solomon, S. 2012. Thermospheric Density: An Overview of Temporal and Spatial
 356 Variations. *Space Science Reviews*, 168(1), p.147–173.

357 Qian, L., and Yue, J. 2017. Impact of the lower thermospheric winter-to-summer residual circulation
 358 on thermospheric composition. *Geophys. Res. Lett.*, 44(9), p.3971-3979.
 359 doi:10.1002/2017GL073361.

360 Qian, L., Burns, A. G., Solomon, S. C., and Wang, W. 2013. Annual/semiannual variation of the
 361 ionosphere. *Geophys. Res. Lett.*, 40(10), p.1928-1933. doi: <https://doi.org/10.1002/grl.50448>.

362 Qian, L., Gan, Q., Wang, W., Cai, X., Eastes, R., and Yue, J. 2022. Seasonal Variation of
 363 Thermospheric Composition Observed by NASA GOLD. *Journal of Geophysical Research: Space
 364 Physics*, 127(6). doi: <https://doi.org/10.1029/2022JA030496>.

365 Qian, L., Solomon, S. C., and Kane, T. J. 2009. Seasonal variation of thermospheric density and
 366 composition. *Journal of Geophysical Research: Space Physics*, 114(A1). doi:
 367 <https://doi.org/10.1029/2008JA013643>

368 Rishbeth, H. 1998. How the thermospheric circulation affects the ionospheric F2-layer. *Journal of
 369 Atmospheric and Solar-Terrestrial Physics*, 60(14), p.1385-1402. doi:
 370 [https://doi.org/10.1016/S1364-6826\(98\)00062-5](https://doi.org/10.1016/S1364-6826(98)00062-5).

371 Sassi, F., McCormack, J., and McDonald, S. 2019. Whole Atmosphere Coupling on Intraseasonal
 372 and Interseasonal Time Scales: A Potential Source of Increased Predictive Capability. *Radio
 373 Science*, 54(11), p.913-933. doi: <https://doi.org/10.1029/2019RS006847>

374 Solomon, S., Liu, H.L., Marsh, D., McInerney, J., Qian, L., and Vitt, F. 2019. Whole Atmosphere
 375 Climate Change: Dependence on Solar Activity. *Journal of Geophysical Research: Space
 376 Physics*, 124(5), p.3799-3809. doi: <https://doi.org/10.1029/2019JA026678>.

377 Thayer, J., Tobiska, W., Pilinski, M., and Sutton, E. (2021) 'Remaining Issues in Upper Atmosphere
 378 Satellite Drag', *Space Weather Effects and Applications*. American Geophysical Union (AGU),
 379 σσ. 111–140. doi: 10.1002/9781119815570.ch5. doi:
 380 <https://doi.org/10.1002/9781119815570.ch5>.

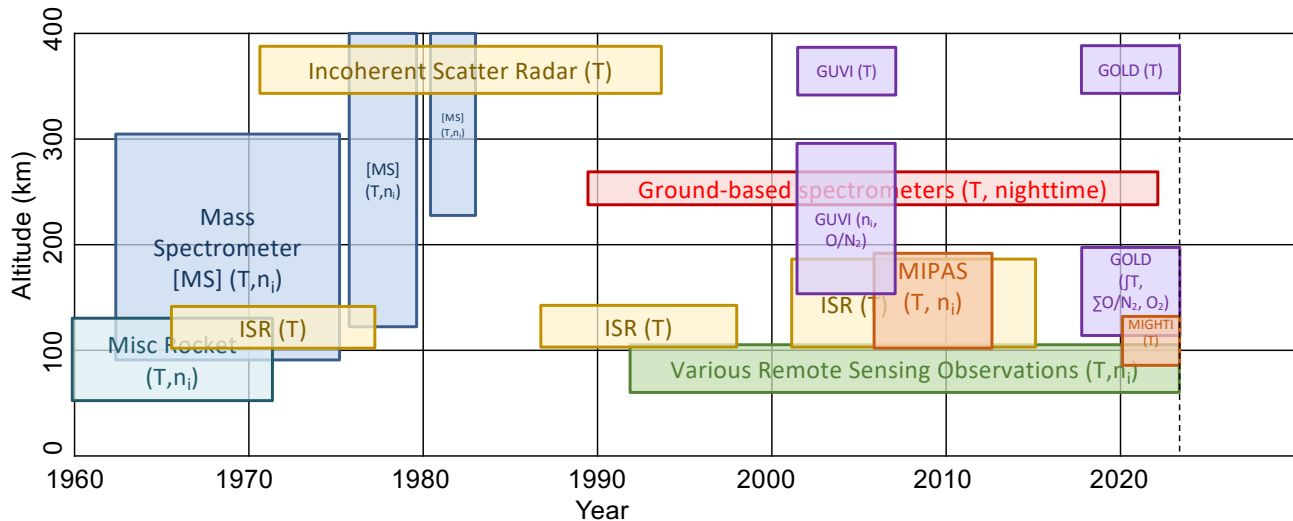
381 Vadas, S., Liu, H.L., and Lieberman, R. 2014. Numerical modeling of the global changes to the
 382 thermosphere and ionosphere from the dissipation of gravity waves from deep
 383 convection. *Journal of Geophysical Research: Space Physics*, 119(9), p.7762-7793.
 384 doi:10.1002/2014JA020280.

385 Yamazaki, Y., and Richmond, A. 2013. A theory of ionospheric response to upward-propagating
 386 tides: Electrodynamic effects and tidal mixing effects. *Journal of Geophysical Research: Space
 387 Physics*, 118(9), p.5891-5905. doi:10.1002/jgra.50487

388 Yuan, T., Stevens, M., Englert, C., and Immel, T. 2021. Temperature Tides Across the Mid-Latitude
 389 Summer Turbopause Measured by a Sodium Lidar and MIGHTI/ICON. *Journal of Geophysical
 390 Research: Atmospheres*, 126(16). doi: <https://doi.org/10.1029/2021JD035321>

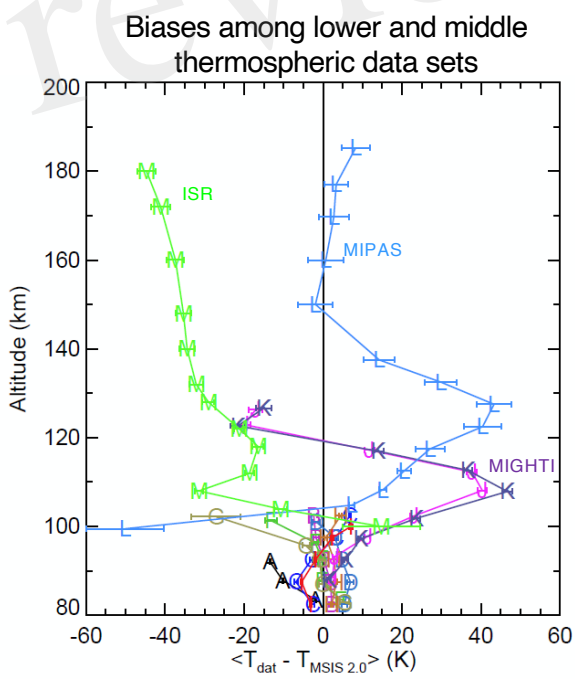
391 Yue, J., Wang, W., Ruan, H., Chang, L., and Lei, J. 2016. Impact of the interaction between the
 392 quasi-2 day wave and tides on the ionosphere and thermosphere. *Journal of Geophysical
 393 Research: Space Physics*, 121(4), p.3555-3563. doi:10.1002/2016ja022444

394
 395
 396
 397
 398
 399



401 **Figure 1.** Coverage of existing and historical thermospheric composition and temperature data sets in
402 terms of altitude and year. Note that the amount of data available within these ranges varies widely,
403 and is generally very sparse. The dashed line indicates present day.

404



405

406 **Figure 2.** Biases among selected lower and middle thermospheric temperature datasets, during
407 daytime and at mid-latitudes (30S – 47N) with respect to NRLMSIS 2.0 as the baseline.. The middle
408 thermospheric data sets MIGHTI (“J”, “K”), MIPAS (“L”), and ground-based incoherent scatter radar
409 (ISR, “M”) are highlighted. The data sets below 100 km include a variety of space-based and ground-
410 based remote sensing measurements. Error bars denote the statistical uncertainty of the estimated
411 biases. Also shown but not discussed in are AURA/MLS (“A”), ACE/FTS (“B”), UARS/HALOE
412 (“C”), AIM/SOFIE (“D”), Boulder, CO Lidar (“E”), Ft. Collins, CO Lidar (“F”), Logan, UT Lidar
413 (“G”), TIMED/SABER (“H”), and ODIN/OSIRIS (“I”).

414

Observable	Coverage
T(z)	<i>Horizontal: Global @ 500 km resolution</i>
O(z), O ₂ (z), N ₂ (z), H(z), He(z)	<i>Vertical: 100-300 km @ 5 km resolution</i> <i>Time: 24 hours @ 4 but preferably 6 local times</i>

415 **Table 1.** Key thermospheric composition and temperature observables between 100-200 km.

416 **FIGURE CAPTIONS**

417 **Figure 1.** Coverage of existing and historical thermospheric composition and temperature data sets in
418 terms of altitude and year. Note that the amount of data available within these ranges varies widely,
419 and is generally very sparse. The dashed line indicates present day.

420 **Figure 2.** Biases among selected lower and middle thermospheric temperature datasets, during
421 daytime and at mid-latitudes (30S – 47N) with respect to NRLMSIS 2.0 as the baseline.. The middle
422 thermospheric data sets MIGHTI (“J”, “K”), MIPAS (“L”), and ground-based incoherent scatter radar
423 (ISR, “M”) are highlighted. The data sets below 100 km include a variety of space-based and ground-
424 based remote sensing measurements. Error bars denote the statistical uncertainty of the estimated
425 biases. Also shown but not discussed in are AURA/MLS (“A”), ACE/FTS (“B”), UARS/HALEO
426 (“C”), AIM/SOFIE (“D”), Boulder, CO Lidar (“E”), Ft. Collins, CO Lidar (“F”), Logan, UT Lidar
427 (“G”), TIMED/SABER (“H”), and ODIN/OSIRIS (“I”).

428 **Table 1.** Key thermospheric composition and temperature observables between 100-200 km.

Figure 1.JPG

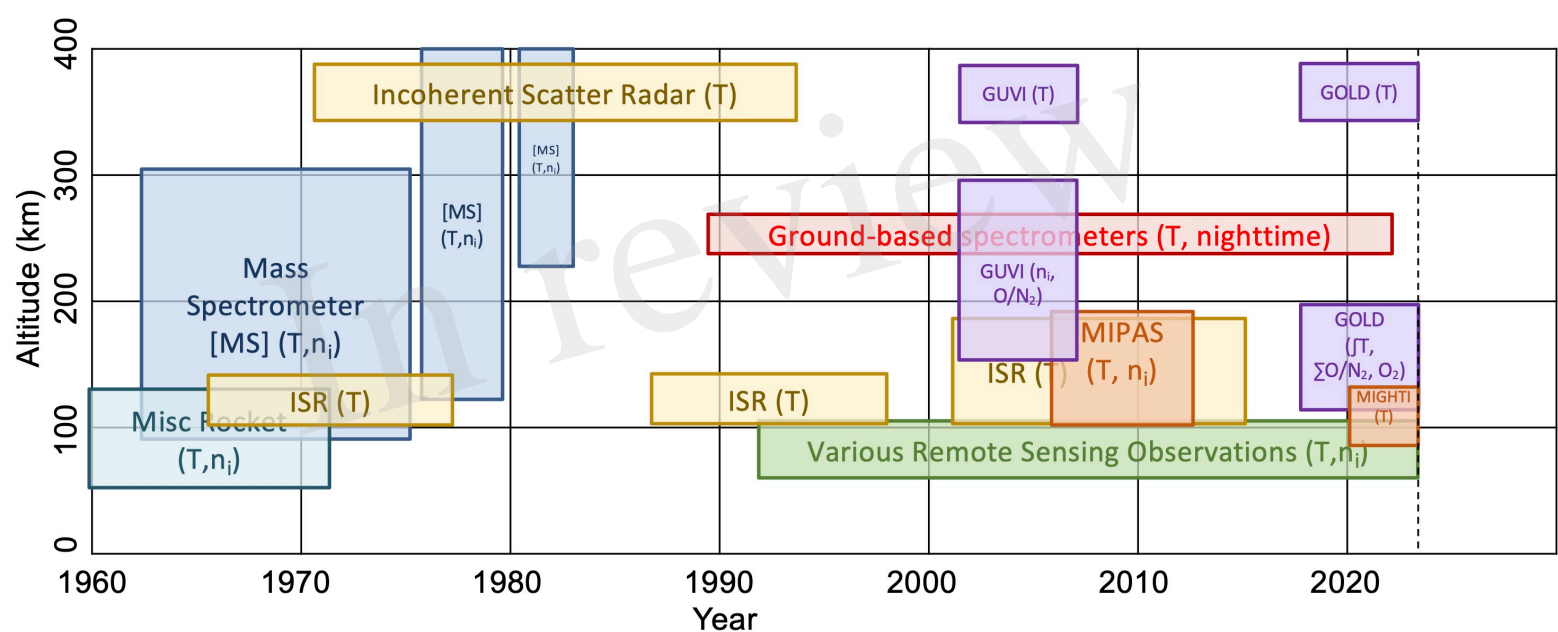


Figure 2.JPEG

Biases among lower and middle thermospheric data sets

